A New Approach for Molecular Electronic Junctions with a Multilayer Graphene Electrode

*Gunuk Wang, Yonghun Kim, Minhyeok Choe, Tae-Wook Kim, and Takhee Lee**

Interest in the field of molecular electronics is grounded in the fact that devices based on molecules constitute the ultimate device miniaturization limit that both inorganic- and organic-based electronics aspire to reach.[1–10] The non-linear current–voltage characteristics of molecular junctions have been extensively investigated with a variety of platforms and techniques, such as scanning probe microscope-based techniques,[10–13] break junctions,[5,14–17] crossed-wire tunnel junctions,[18–20] and various solid-state device-based methods.[4,6,21–25] Within these efforts, the creation of a stable solid-state molecular junction has been a long-standing challenge in terms of understanding molecular charge transport mechanisms and practical device applications. Most fabrication techniques involve evaporating a metal onto the molecules as the top electrode.[21–24,26,27] This process causes electrical short circuits and unstable and unexpected current–voltage characteristics due to filamentary paths and damage to the molecules.[22,23,26–29] These inevitable uncertainties in the fabrication technique lead to relatively large variations in the junction conductance, despite the use of identical molecular components, and this is an obstacle for truly understanding molecular charge transport mechanisms and device applications. New techniques and ideas have been developed to resolve this issue.[4,6,21,30,31] The fabrication of molecular junctions using a conductive polymer (PEDOT:PSS) between the top electrode and the molecules has been one of the most successful techniques in terms of high device yields and stable junctions.[21] Nevertheless, the use of a conductive polymer has some limitations and presents some uncertainties as a platform for physical-organic studies, because the properties of the interface between the polymer layer and the molecules are not well-understood.[21,30–33] For example, it has been reported that the resistance of the materials fabricated using this technique is significantly different to those of molecular junctions that do not have the polymer interlayer[30–33] due to poor contact between PEDOT:PSS and the molecules. Additionally, the yield of the polymer-based junction system seems to depend on the type of isolating layer (photoresist or SiO_2)[21,33] and on the molecular contact groups (hydrophilic or hydrophobic)[21] due to differences in the surface tension. Because of these limitations, the PEDOT:PSS-based molecular device approach may be limited in its ability to characterize the charge transport of molecular systems with a wide range of different contacts (hydrophilic and hydrophobic) and various molecular lengths. Therefore, although the fabrication of PEDOT:PSS-based molecular electronic devices has been excellent for producing high-yield molecular devices, there is still a need to find alternative solid-state molecular device structures beyond the PEDOT:PSS-based molecular structure.

Graphene is a ultra-thin two-dimensional sheet of covalently bonded carbon atoms with outstanding electronic properties, chemical stability and mechanical material properties.[34–37] It is considered to be a good electrode candidate for molecular junctions. Furthermore, large-area, conductive and flexible graphene films have been successfully synthesized, with the ability to patterning or creation of a desired size and shape of the film.[38,39] For this reason, graphene films have the potential to play a crucial role as a conductive electrode for organic electronic devices. For example, many studies have reported graphene electrodes in organic-based devices such as memories,[40] filed-effect transistors,[41] light-emitting diodes,[42] and solar cell devices.[43]

In this paper, we introduce a new approach for fabricating reliable solid-state molecular devices using a graphene electrode as the top electrode and show that these devices have a resistance per molecule comparable to that of pure metal–molecule–metal devices. In particular, this new method produces excellent durability, thermal and operational stability, and device lifetimes. Additionally, the yield of graphene-based molecular devices was found to be approximately 90%, regardless of the properties of the isolating layer and the contact groups (hydrophobic vs hydrophilic). The properties of the interface between graphene and the molecules were statistically investigated. This new approach is a reliable platform for the practical characterization and application of molecular junctions.

Figure 1 shows schematic diagrams of the process of fabricating molecular junctions using the molecular components investigated in this study. We chose alkyl-based molecules in our new device system because the transport behavior through alkyl-based molecules has been extensively investigated using various types of molecular systems. Many research groups have used alkyl-based molecules for their junction structures in scanning tunneling microscopy (STM),[12] conductive-probe atomic force microscopy (CP-AFM),[44] nanogaps,[14,45]

G. Wang, Y. Kim, M. Choe, Dr. T.-W. Kim,[+] Prof. T. Lee
Department of Materials Science and Engineering
Gwangju Institute of Science and Technology
Oryong-Dong, Buk-Gu, Gwangju 500–712, Korea
E-mail: tlee@gist.ac.kr
Prof. T. Lee
Department of NanobioMaterials and Electronics
Gwangju Institute of Science and Technology
Oryong-Dong, Buk-Gu, Gwangju 500–712, Korea
[+]Present Address: Korea Institute of Science and Technology
Institute of Advanced Composite Materials
Jeollabuk-do, 565–902, Korea

DOI: 10.1002/adma.201003178

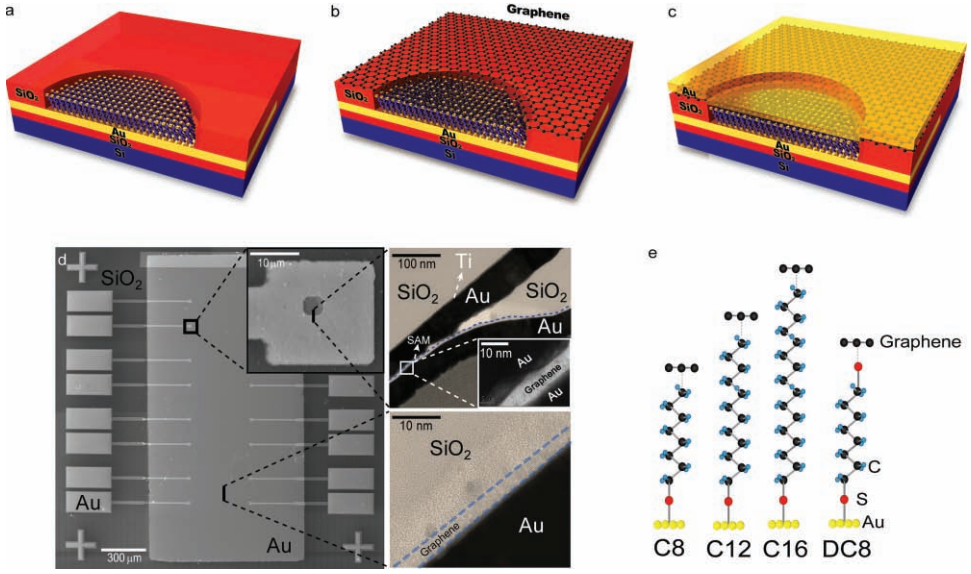

Figure 1. a) Deposition of alkanethiol SAM on the exposed Au bottom electrode. b) Alkanethiol SAM sandwiched between the Au bottom electrode and the graphene film as the top electrode. c) The junction was completed by Au vapor-deposition through a shadow mask. d) SEM and TEM images of the devices: the right images show cross-sectional TEM images of the active and non-active regions of the molecular junctions. e) The four types of studied molecular systems along with their chemical structures: C8, C12, C16, and DC8.

nanopores,[24] and microscale devices.[21,22] From this point of view, the use of alkyl-based molecules is important and provides a clear criterion for whether any new device structure can be a good test platform for molecular systems. The alkanethiol molecular species used in our study were octanethiol (denoted as C8), dodecanethiol (C12), hexadecanethiol (C16) and octanedithiol (DC8) (Figure 1e). After the alkanethiols were self-assembled on an exposed 4 μm diameter Au-bottom electrode (Figure 1a), a multilayer graphene film (thickness less than approximately 10 nm) was transferred to the substrate as the top electrode (Figure 1b and cross-sectional transmission electron microscopy (TEM) images in Figure 1d). We prepared multilayer graphene (MLG) films by chemical vapor deposition (CVD)[42] (see the Supporting Information). The growth mechanism of CVD-grown graphene on the Ni film is the segregation and precipitation of carbon atoms that are dissolved and saturated into the Ni film at high temperature, forming a graphene film during the cooling stage.[46] For uniform graphene growth by the CVD method, it is important to control the temperature, gas composition and cooling rate. In a previous work, we charaterized CVD-grown MLG film and fabricated electronic devices such as light emitting diodes, photovoltaic cells and transistors.[42,47,48] The MLG films prepared at a growth temperature of 1 000 °C showed a sheet resistance of around 600 Ω per square and a transmittance of around 87% in the visible wavelength range. Also the thinnest graphene thickness is typically around 1 nm from atomic force microscopy (AFM) images. Next, an Au layer was vapor-deposited on top of the graphene films using a shadow mask at a low deposition rate (0.1 Å s^{-1}) to reduce the sheet resistance of the graphene films during electrical probing (Figure 1c). The graphene interlayer electrode prevents the formation of electrical shorts and filamentary paths that would result from penetration of the Au top metal (TEM images in Figure 1d). The fabrication of the molecular devices was completed by reactive ion etching to remove the redundant graphene films on the devices.

We fabricated and characterized a number of molecular devices to statistically analyze the molecular electronic properties. Based on statistical criteria,[22] we observed a remarkable improvement in the yield of working molecular devices using the graphene top electrode (yield of around 90%) compared to molecular devices without any interlayer (yield < 2%).[22,49] The yield of PEDOT:PSS molecular junctions with an isolating layer of SiO_2 (hydrophobic) was found to be much smaller (yield ≈ 58%)[33] than those of devices using an isolating photoresist layer (hydrophilic) (yield ≈ 95%),[21] which is due to the difference in surface tension between the two cases. However, we demonstrate here that the yield of graphene-based molecular devices is not strongly affected by the properties of the isolating layer and top contact groups (hydrophobic vs. hydrophilic). We found high device yields for both C8 (around 88%) and DC8 (around 98%) junctions, even with the SiO_2 isolating layer. The detailed yields of the working molecular devices are provided in Table S1 in the Supporting Information.

Figure 2a shows the statistical current density–voltage (*J*–*V*) data measured for the alkanemonothiol (C8, C12, and C16) and alkanedithiol (DC8) molecular junctions with graphene electrodes. The error bars were obtained from the corresponding log-standard deviations of the individual working devices. These graphs show that the current density was exponentially dependent on the length of the alkanemonothiols. This result suggests that tunneling is the main conduction mechanism.[22] Tunneling conduction was verified by the temperature-independent *J*–*V* characteristics (Figure S2 in the Supporting Information).[22] The *J*–*V* characteristics depend on the molecular length (C8, C12, and C16) and the graphene-molecule contacts (i.e., monothiol vs. dithiol). The difference in the conductances

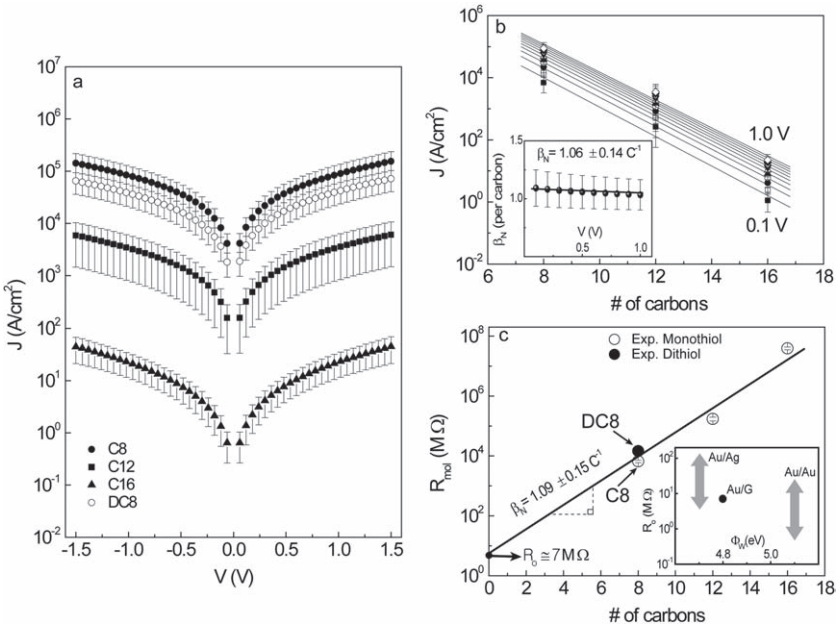

Figure 2. a) Statistical *J–V* data for all C8, C12, C16 and DC8 molecular devices. b) A semi-log plot of *J* at different biases versus the number of carbon atoms in the molecules of C8, C12 and C16 devices; the solid lines are the exponential fitting results, which give β_N as a function of the applied bias (inset in Figure 2b). c) A semi-log plot of the resistance per molecule (R_{mol}) versus the number of carbon atoms in the molecules of C8, C12, C16 and DC8 devices; the inset shows the experimental contact resistance (R_o), in which the grey arrows represent the range of the R_o values reported in the literature.[32,44,49–51] The symbol Φ_W (eV) represents the average work functions of the electrodes (around 4.8 eV for [Au/graphene]).

of C8 and DC8 (with C8 having a higher conductance than of DC8 junctions) cannot be explained by their typical metal–molecule contact properties (physisorbed vs. chemisorbed contacts) at the Au-molecule contacts.[22,32,44,49–51] Because the graphene electrode does not form a chemisorbed contact with thiol [–S], the difference in the conductance between the C8 and DC8 junctions can only be explained by a difference in the properties of the physisorbed contacts corresponding to different contact lengths. Additionally, the DC8 self-assembled monolayer (SAM) has the same ordering structure (tilt angle and packing density) as the C8 SAM on Au (111) based on molecular-resolution STM images.[52] Thus, the conductance of the C8 junction is higher than that of the DC8 junction because of the shorter contact length in the C8 junction (contact length $d_{[CH3/graphene]}$ for C8 < $d_{[C\text{-}S/graphene]}$ for DC8). However, the fluctuation of the tilt angle and packing on the Au substrate could result in statistical variation in the conductance measurement.

The statistics obtained from a large number of working molecular junctions allowed for a better interpretation of the electrical transport through the molecular tunnel barrier.[4,6,22,30–33,44,49,53] Figure 2b is a semi-log plot of *J* measured from 0.1 to 1.0 V as a function of the number of carbon atoms in the molecules. The tunneling current density *J* shows an exponential dependence [$J \propto \exp(-\beta_N N)$] on the number of carbons atoms (*N*) in the alkyl chain.[21,22,30,32,44,49–51] The decay coefficient per carbon atom (β_N) was determined from linear fits at different biases. β_N reflects the extent of the decrease in the wave function of the tunneling charge. This β_N is presented as a function of the bias in the inset of Figure 2a. The value of β_N obtained was 1.06 ± 0.14 C^{-1} (0.85 ± 0.11 $Å^{-1}$), which is in good agreement with previously reported values for alkanethiol junctions.[12,22,32,44,49–51,54] To compare our transport results to other data from the literature, we normalized the resistance to the resistance per single molecule, R_{mol} (MΩ) (Figure S3 in the Supporting Information). Here, R_{mol} is the resistance per molecule obtained from the linear fit of the low-bias statistical current-voltage (*I–V*) data (–0.3 V ≤ *V* ≤ 0.3 V) along with the molecular grafting density (around 4.60×10^{18} m^{-2} for alkanethiols)[21,50,52] and the junction area (1.26×10^{-11} m^2). When R_{mol} is plotted as a function of the number of carbon atoms, the contact resistance R_o can be obtained from the length dependence of the resistance, as shown in Figure 2c. The contact resistance R_o for the Au–SAM/graphene junction was found to be approximately 7 MΩ, which is between the reported R_o values for Au–SAM/Ag[44,51] and Au–SAM/Au junctions[32,44,49–51] (see also the inset of Figure 2c). Generally, the R_o of alkanethiols depends on the work functions of the contact electrodes.[44,51] The work function of multilayer graphene ranges from 4.3 to 4.5 eV, as measured using the Kelvin probe technique in our study. When the top electrode's work function increases, the R_o of alkanethiols decreases due to the reduction in the hole injection barrier height (i.e., hole-type transport in alkanethiols).[44,51]

The durability, operational stability and device lifetime of molecular junctions are often neglected in many studies, but these factors are crucial for the practical application of molecular devices.[6,30,31] **Figure 3**a shows the *J–V* characteristics of the C8, C12, C16 and DC8 molecular junctions. The inset of Figure 3a shows the *J–V* curves for a C8 junction measured immediately after device fabrication and after being stored at ambient conditions for 40 d. The original *J–V* characteristics were preserved without any deterioration during storage. Figure 3b shows the operational stability results obtained by measuring *J* at 1.0 V (the black arrows in Figure 3a) as a function of time. The value of *J* at 1.0 V was retained for 10^4 s (measurement interval Δt = 100 s). Figure 3c shows that the DC8 molecular devices also had good retention (without any significant degradation) of the cross-measured positive current I_+ (at 1.0 V) and the negative current *I*– (at –1.0 V) for 10^4 s with a measurement interval Δt = 5 s. These results demonstrate the excellent reliability of the electrical characteristics of graphene–electrode molecular devices. The graphene interlayer produces highly stable molecular junctions by effectively preventing the diffusion or formation of metallic filaments through the molecular layers, even under repeated voltage stress conditions.

To demonstrate the quality of the contact and the thermal stability of the graphene-based devices, we compared the charge transport parameters (*J* and R_{mol}) and the thermal

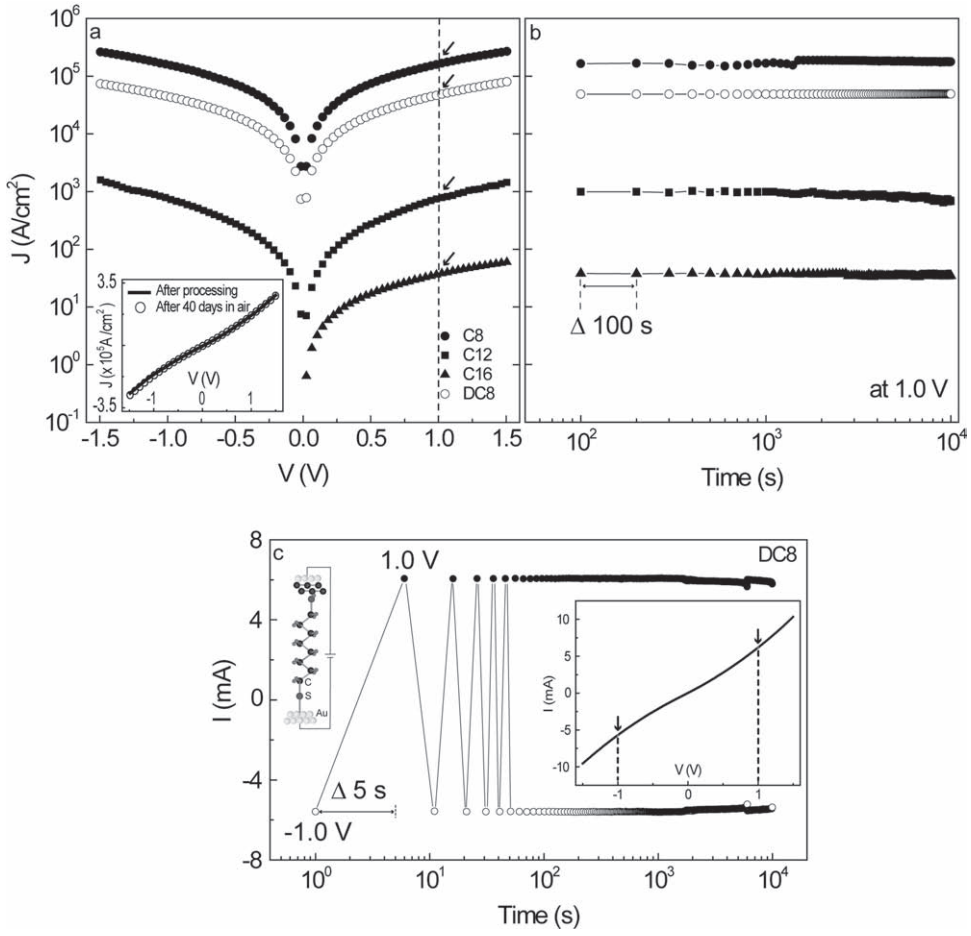

Figure 3. a) The *J–V* characteristics for representative C8, C12, C16 and DC8 molecular devices. The inset shows a DC8 device measured after fabrication (solid line) and after storage at ambient conditions for 40 d (open circles). b) Retention characteristics of the molecular junctions in terms of the measured *J* at 1.0 V for 10^4 s (measurement interval $\Delta t = 100$ s). c) Retention characteristics of the cross-measured positive current (measured at +1.0 V) and negative current (measured at −1.0 V) for 10^4 sec with an interval $\Delta t = 5$ s.

stability for DC8 molecular junctions according to the kind of top electrode (PEDOT:PSS, graphene and Au) based on the statistical analysis of working molecular devices. **Figure 4**a shows the histogram of current densities at 1.0 V on a logarithmic scale, and Figure 4b shows R_{mol} for different kinds of top electrodes. In these comparisons, we observed that the resistance for Au/DC8/graphene was slightly higher than that for Au/DC8/Au devices by less than one order of magnitude (Figure 4b). Unlike the relatively poor contact between DC8 and PEDOT:PSS (with much more resistance in the Au/DC8/PEDOT:PSS case), the contact between graphene and DC8 was comparable to that between Au and DC8 (Figure 4a and b). This difference can also be observed in different types of junction systems. For example, we observed that the R_{mol} (around 10 GΩ) for DC8/graphene devices was higher by 0.5–2 orders of magnitude than were CP-AFM and STM measurements using the same molecular types, due to the physisorbed contact between graphene layers and DC8 molecules.[12,32,44,54] However, the R_{mol} of the devices with PEDOT:PSS was observed[21,32] to be around around 10^3 GΩ, which is much higher than were CP-AFM and STM measurements, by 3–5 orders of magnitude. Thus, it can be said that the junction conductance of PEDOT:PSS-based molecular devices is limited by the low vertical conductance of PEDOT:PSS itself.[55] This leads to a difficulty in characterizing the charge transport through short molecular lengths (<2 nm) in the PEDOT:PSS-based molecular system.[30] Therefore, the approach of graphene-based molecular devices may be advantageous for characterizing a wider range of molecular systems.

Figure 4c shows the R_{mol} for the DC8 junction according to the type of top electrode (PEDOT:PSS and graphene) as a function of temperature from 290 to 383 K. The R_{mol} for the PEDOT:PSS-based DC8 device rapidly decreased with increasing temperature (323 to 383 K), which is consistent with previous results.[56] A phase change of the SAM by molecular desorption or removal of the remaining water from the hydrophilic PEDOT:PSS/molecule interface has been reported to be the main cause of the rapid decrease in the R_{mol} values as the temperature increases.[56] On the other hand, the R_{mol} for the hydrophobic graphene-based DC8 device slowly decreased with increasing temperatures. This result indicates that the graphene-based device has greater thermal stability than the

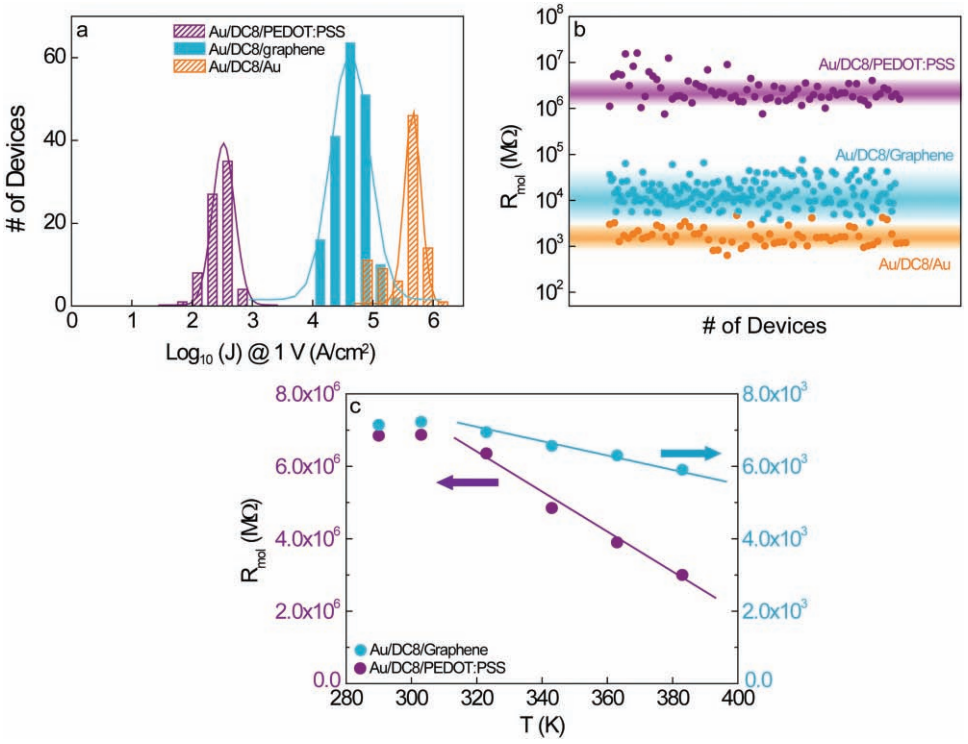

Figure 4. a) Histogram of logarithmic current densities at 1 V for working molecular devices according to the kind of top electrode (PEDOT:PSS, graphene, or Au). b) The resistance per molecule R_{mol} values for these molecular junctions. c) The R_{mol} values for Au/DC8/PEDOT:PSS and Au/DC8/graphene devices as a function of increasing temperature.

PEDOT:PSS-based device, and this factor can be advantageous for operating molecular devices over a wide range of temperatures while maintaining the original transport properties.

In summary, we have demonstrated a new technique for fabricating a solid-state molecular junction with graphene as the top electrode with a high yield of the working molecular devices. As compared with earlier PEDOT:PSS-based molecular devices, graphene-based devices may have potential advantages in terms of proper charge transport characteristics in molecular systems with a wide range of variable lengths and different contacts (hydrophilic and hydrophobic). Additionally, the electronic coupling of graphene to the molecules seems to be better than that for PEDOT:PSS and molecules, resulting in a better contact conductance. In particular, we demonstrated good durabilities, thermal and operational stabilities, and device lifetimes of the graphene-based molecular junctions, all of which are crucial for the practical application of molecular devices.

Supporting Information

Supporting Information is available from the Wiley Online Library or from the author.

Acknowledgements

This work was supported by the National Research Laboratory program, the National Core Research Centre grant, the World Class University program of the Korean Ministry of Education, Science, and Technology, and the Program for Integrated Molecular Systems at Gwangju Institute of Science and Technology.

Received: September 1, 2010
Revised: November 13, 2010
Published online: December 17, 2010

[1] A. Aviram, M. A. Ratner, *Chem. Phys. Lett.* **1974**, *29*, 277.
[2] A. Nitzan, M. A. Ratner, *Science* **2003**, *300*, 1384.
[3] J. C. Love, L. A. Estroff, J. K. Kriebel, R. G. Nuzzo, G. M. Whitesides, *Chem. Rev.* **2005**, *105*, 1103.
[4] J. Chen, M. A. Reed, A. M. Rawlett, J. M. Tour, *Science* **1999**, *286*, 1550.
[5] M. A. Reed, C. Zhou, C. J. Muller, T. P. Burgin, J. M. Tour, *Science* **1997**, *278*, 252.
[6] J. E. Green, J. Wook Choi, A. Boukai, Y. Bunimovich, E. Johnston-Halperin, E. DeIonno, Y. Luo, B. A. Sheriff, K. Xu, Y. Shik Shin, H.-R. Tseng, J. F. Stoddart, J. R. Heath, *Nature* **2007**, *445*, 414.
[7] B. Behin-Aein, D. Datta, S. Salahuddin, S. Datta, *Nat. Nanotechnol.* **2010**, *5*, 266.
[8] M.-P. Kasper, B. Thomas, *Nat. Nanotechnol.* **2009**, *4*, 551.
[9] M. Galperin, M. A. Ratner, A. Nitzan, A. Troisi, *Science* **2008**, *319*, 1056.
[10] L. Lafferentz, F. Ample, H. Yu, S. Hecht, C. Joachim, L. Grill, *Science* **2009**, *323*, 1193.
[11] L. Venkataraman, J. E. Klare, C. Nuckolls, M. S. Hybertsen, M. L. Steigerwald, *Nature* **2006**, *442*, 904.
[12] B. Xu, N. J. Tao, *Science* **2003**, *301*, 1221.
[13] S. Ho Choi, B. Kim, C. D. Frisbie, *Science* **2008**, *320*, 1482.

[14] H. Song, Y. Kim, Y. H. Jang, H. Jeong, M. A. Reed, T. Lee, *Nature* **2009**, *462*, 1039.
[15] X. Chen, S. Yeganeh, L. Qin, S. Li, C. Xue, A. B. Braunschweig, G. C. Schatz, M. A. Ratner, C. A. Mirkin, *Nano Lett.* **2009**, *9*, 3974.
[16] J. Park, A. N. Pasupathy, J. I. Goldsmith, C. Chang, Y. Yaish, J. R. Petta, M. Rinkoski, J. P. Sethna, H. D. Abruna, P. L. McEuen, D. C. Ralph, *Nature* **2002**, *417*, 722.
[17] W. Liang, M. P. Shores, M. Bockrath, J. R. Long, H. Park, *Nature* **2002**, *417*, 725.
[18] J. G. Kushmerick, D. B. Holt, J. C. Yang, J. Naciri, M. H. Moore, R. Shashidhar, *Phys. Rev. Lett.* **2002**, *89*, 086802.
[19] J. G. Kushmerick, J. Naciri, J. C. Yang, R. Shashidhar, *Nano Lett.* **2003**, *3*, 897.
[20] J. G. Kushmerick, J. Lazorcik, C. H. Patterson, R. Shashidhar, D. S. Seferos, G. C. Bazan, *Nano Lett.* **2004**, *4*, 639.
[21] H. B. Akkerman, P. W. M. Blom, D. M. de Leeuw, B. de Boer, *Nature* **2006**, *441*, 69.
[22] T.-W. Kim, G. Wang, H. Lee, T. Lee, *Nanotechnology* **2007**, *18*, 315204.
[23] H. Haick, D. Cahen, *Acc. Chem. Res.* **2008**, *41*, 359.
[24] W. Wang, T. Lee, I. Kretzschmar, M. A. Reed, *Nano Lett.* **2004**, *4*, 643.
[25] Y.-L. Loo, D. V. Lang, J. A. Rogers, J. W. P. Hsu, *Nano Lett.* **2003**, *3*, 913.
[26] B. de Boer, M. M. Frank, Y. J. Chabal, W. Jiang, E. Garfunkel, Z. Bao, *Langmuir* **2004**, *20*, 1539.
[27] H. Haick, O. Niitsoo, J. Ghabboun, D. Cahen, *J. Phys. Chem. C* **2007**, *111*, 2318.
[28] A. V. Walker, T. B. Tighe, O. M. Cabarcos, M. D. Reinard, B. C. Haynie, S. Uppili, N. Winograd, D. L. Allara, *J. Am. Chem. Soc.* **2004**, *126*, 3954.
[29] G. L. Fisher, A. V. Walker, A. E. Hooper, T. B. Tighe, K. B. Bahnck, H. T. Skriba, M. D. Reinard, B. C. Haynie, R. L. Opila, N. Winograd, D. L. Allara, *J. Am. Chem. Soc.* **2002**, *124*, 5528.
[30] P. A. Van Hal, E. C. P. Smits, T. C. T. Geuns, H. B. Akkerman, B. C. De Brito, S. Perissinotto, G. Lanzani, A. J. Kronemeijer, V. Geskin, J. Cornil, P. W. M. Blom, B. De Boer, D. M. De Leeuw, *Nat. Nanotechnol.* **2008**, *3*, 749.
[31] C. A. Nijhuis, W. F. Reus, G. M. Whitesides, *J. Am. Chem. Soc.* **2009**, *131*, 17814.
[32] H. B. Akkerman, B. de Boer, *J. Phys.: Condens. Matter* **2008**, *20*, 013001.
[33] G. Wang, H. Yoo, S.-I. Na, T.-W. Kim, B. Cho, D.-Y. Kim, T. Lee, *Thin Solid Films* **2009**, *518*, 824.
[34] K. S. Novoselov, A. K. Geim, S. V. Morozov, D. Jiang, Y. Zhang, S. V. Dubonos, I. V. Grigorieva, A. A. Firsov, *Science* **2004**, *306*, 666.
[35] I. Meric, M. Y. Han, A. F. Young, B. Ozyilmaz, P. Kim, K. L. Shepard, *Nat. Nanotechnol.* **2008**, *3*, 654.
[36] Y. Zhang, J. W. Tan, H. L. Stormer, P. Kim, *Nature* **2005**, *438*, 201.
[37] Q. H. Wang, M. C. Hersam, *Nat. Chem.* **2009**, *1*, 206.
[38] K. S. Kim, Y. Zhao, H. Jang, S. Y. Lee, J. M. Kim, K. S. Kim, J.-H. Ahn, P. Kim, J.-Y. Choi, B. H. Hong, *Nature* **2009**, *457*, 706.
[39] A. Reina, X. Jia, J. Ho, D. Nezich, H. Son, V. Bulovic, M. S. Dresselhaus, J. Kong, *Nano Lett.* **2008**, *9*, 30.
[40] J. Liu, Z. Yin, X. Cao, F. Zhao, A. Lin, L. Xie, Q. Fan, F. Boey, H. Zhang, W. Huang, *ACS Nano* **2010**, *4*, 3987.
[41] C.-A . Di, D. Wei, G. Yu, Y. Liu, Y. Guo, D. Zhu, *Adv. Mater.* **2008**, *20*, 3289.
[42] G. Jo, M. Choe, C.-Y. Cho, J. H. Kim, W. Park, S. Lee, W.-K. Hong, T.-W. Kim, S.-J. Park, B. H. Hong, Y. H. Kahng, T. Lee, *Nanotechnology* **2010**, *21*, 175201.
[43] X. Wang, L. Zhi, K. Müllen, *Nano Lett.* **2008**, *8*, 323.
[44] V. B. Engelkes, J. M. Beebe, C. D. Frisbie, *J. Am. Chem. Soc.* **2004**, *126*, 14287.
[45] C. Chu, J.-S. Na, G. N. Parsons, *J. Am. Chem. Soc.* **2007**, *129*, 2287.
[46] Q. Yu, J. Lian, S. Siriponglert, H. Li, Y. P. Chen, S.-S. Pei, *Appl. Phys. Lett.* **2008**, *93*, 113103.
[47] M. Choe, B. H. Lee, G. Jo, J. Park, W. Park, S. Lee, W.-K. Hong, M.-J. Seong, Y. H. Kahng, K. Lee, T. Lee, *Org. Electron.* **2010**, *11*, 1864.
[48] S. Lee, G. Jo, S-J. Kang, G. Wang, M. Choe, W. Park, D-Y. Kim, Y. H. Kahng, T. Lee, *Adv. Mater.* **2010**, DOI: 10.1002/adma.201003165.
[49] G. Wang, T.-W. Kim, H. Lee, T. Lee, *Phys. Rev. B* **2007**, *76*, 205320.
[50] A. Salomon, D. Cahen, S. Lindsay, J. Tomfohr, V. B. Engelkes, C. D. Frisbie, *Adv. Mater.* **2003**, *15*, 1881.
[51] G. Wang, T.-K. Kim, Y. H. Jang, T. Lee, *J. Phys. Chem. C* **2008**, *112*, 13010.
[52] K. Seo, H. Lee, *ACS Nano* **2009**, *3*, 2469.
[53] E. Lörtscher, H. B. Weber, H. Riel. *Phys. Rev. Lett.* **2007**, *98*, 176807.
[54] F. Chen, X. Li, J. Hihath, Z. Huang, N. Tao *J. Am. Chem. Soc.* **2006**, *128*, 15874.
[55] A. M. Nardes, M. Kemerink, R. A. J. Janssen, *Phys. Rev. B* **2007**, *76*, 085208.
[56] H. B. Akkerman, A. J. Kronemeijer, J. Harkema, P. A. van Hal, E. C. P. Smits, D. M. de Leeuw, P. W. M. Blom, *Org. Electron.* **2010**, *11*, 146.